

Title	Structural Investigation of Hydrogen in Calcium Silicate and Fluorosilicate Slags
Author(s)	Iwamoto, Nobuya; Makino, Yukio; Kishi, Katsuhiro
Citation	Transactions of JWRI. 10(1) P.63-P.70
Issue Date	1981-03
Text Version	publisher
URL	http://hdl.handle.net/11094/11594
DOI	
rights	本文データはCiNiiから複製したものである
Note	

Osaka University Knowledge Archive : OUKA

<https://ir.library.osaka-u.ac.jp/repo/ouka/all/>

Structural Investigation of Hydrogen in Calcium Silicate and Fluorosilicate Slags †

Nobuya IWAMOTO*, Yukio MAKINO** and Katsuhiko KISHI***

Abstract

Hydrogen absorption of lime-silicate and -fluorosilicate slags, which were produced at 1600°C under Ar + water vapor ($P_{H_2} = 0.128$ atm.) atmosphere, was investigated. State of hydrogen in these slags was also investigated by infrared absorption method. In lime silicate slag, a minimum was observed near 50 mol% SiO₂ in the dependence of total hydrogen content on slag composition. Three absorption bands were observed at 2.9 μ (band 1), 3.4 μ (band 2) and 4.2 μ (band 3) as the result of resolving every corrected absorption spectrum by computer calculation. These three bands were assigned to nearly free hydroxyl and hydroxyls of OH...O⁻ and OH...O^o types from the dependence of each band on slag composition. Three absorption bands in calcium fluorsilicate slags were observed at similar positions. CaF₂ addition to lime silicate slags was effective to lowering hydrogen absorption into the slags when its content was about 7 mol% or over. In calcium fluorosilicate slags with high initial CaF₂ content, however, CaF₂ addition showed harmful effect to lowering hydrogen content in the slags on account of formation of active non-bridged oxygen when CaF₂ content became less than 7 mol% or so.

KEY WORDS: (Hydrogen absorption), (Fluorosilicate Slag)

1. Introduction

Hydrogen in steel causes very harmful effects on mechanical properties of steel such as delayed fracture and hydrogen embrittlement. It is important to prevent hydrogen transferring from atmosphere to molten steel during refinement of steel or welding, so that it is desired to develop the excellent slags (or fluxes) with a very low permeability for hydrogen. Investigations on permeability and diffusion phenomena of hydrogen in glass have often been reported.^{1), 2)} In metallurgical slag, solubility of hydrogen has been measured^{3), 4)} but study on its permeability and diffusion phenomena has scarcely been reported. In this study, the solubility of hydrogen in CaO-SiO₂ slags was investigated by gas chromatric analysis. Subsequently, state of hydrogen in the same slags was determined by the measurement of infrared absorption and differential thermal analysis (DTA), taking into consideration silicate structure. It is well known that the addition of CaF₂ to welding fluxes is effective of decreasing hydrogen and oxygen content in weld metals, so that hydrogen solubility and its structure in calcium fluoro-silicate slags were also investigated.

2. Experimental

Specimen slags were prepared from reagent grade

CaCO₃, SiO₂ and CaF₂. These reagents were accurately weighed and mixed in an agate mortar and pestle. These mixed reagents were melted in platinum crucibles in argon saturated with water vapor. The partial pressure of water vapor in argon was fixed to be 0.128 atm. (97.3 mmHg) in every experiment, using water saturator which regulated the temperature of water within the accuracy of ± 0.1°C. The mixed gas was led into an alumina reaction tube using a gas purifier as shown in Fig. 1. All specimens were quenched by taking into air after these were held for 3 hr at 1600°C except the specimens for examining the dependence of hydrogen absorption on reaction time. All slags were vitrified by air-quenching. Glassy slags were polished by emery papers and buffed by alumina powders for infrared absorption measurement. Infrared absorption spectra were measured in the wavelength range from 2.5 μ to 5.0 μ using a spectrometer of Hitachi 260-50 type. Hydrogen contents of all slags were analyzed by a hydrogen determinator of LECO RH-1E type. DTA curves of several slags were measured in the range from room temperature to 900°C using a balance of Rigaku DGC1H type. α-Al₂O₃ was selected as the standard material. All DTA measurements were performed at the sensitivity of 25 μV and the heating rate of 5°C/min or 10°C/min. Fluorine contents in fluorosilicate slags were determined by X-ray fluorescence method.

† Received on March 31, 1981

* Professor

** Instructor

*** Graduate Student (Osaka University)

Transactions of JWRI is published by Welding Research Institute of Osaka University, Suita, Osaka, Japan

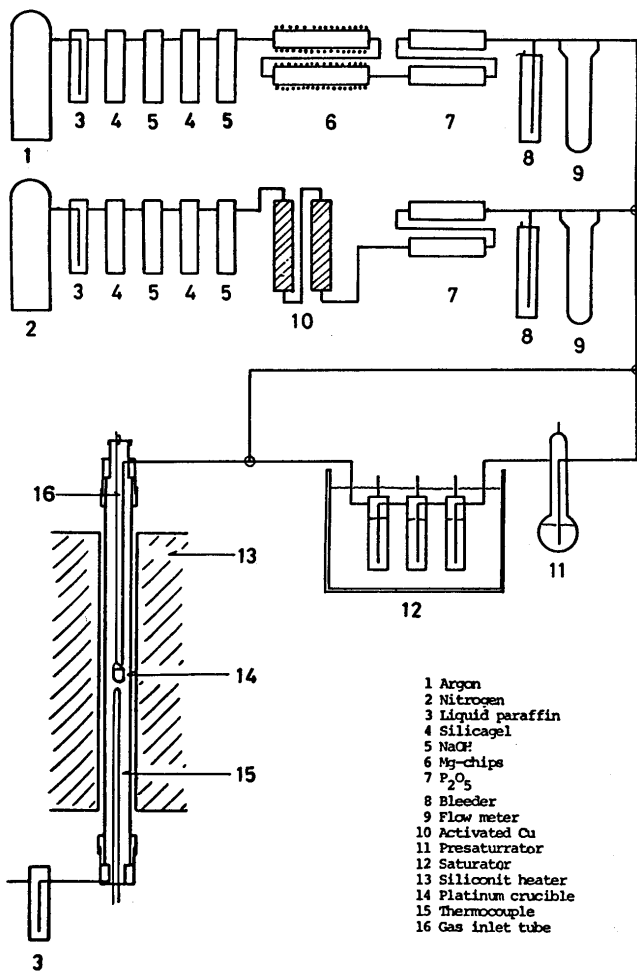
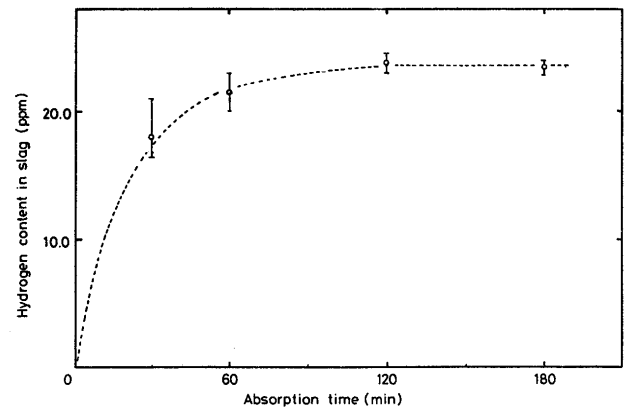
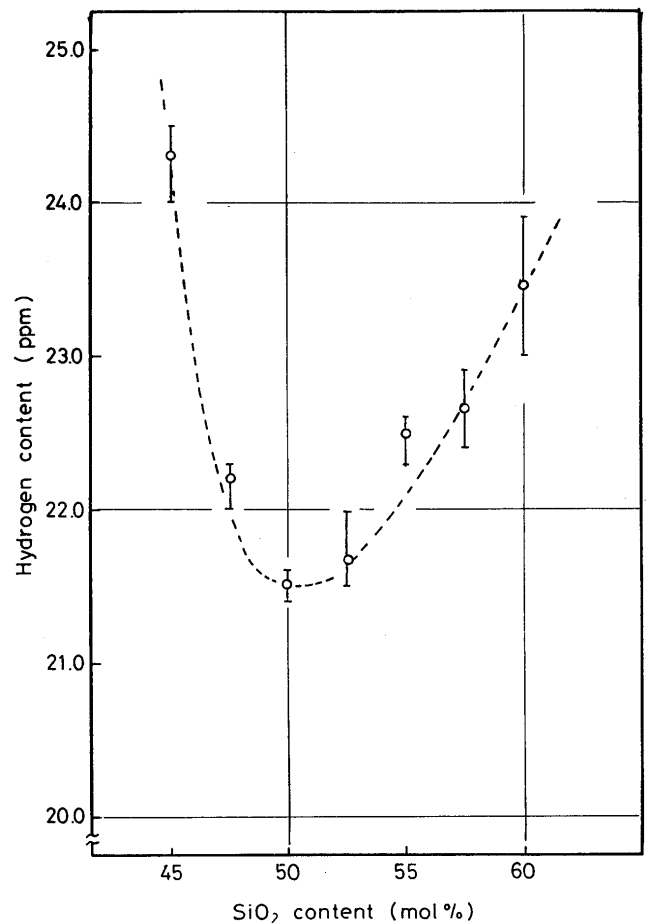


Fig. 1 Experimental apparatus.

3. Results

3.1 CaO-SiO₂ binary slag

Because the viscosity of the slag with $\text{CaO/SiO}_2 = 4/6$ is highest among the slags used in this study, the evaluation of equilibrium time for hydrogen absorption was performed using the slag. As shown in Fig. 2, the dissolution of hydrogen reached the equilibrium at 2 hr at least, so that the holding time for hydrogen dissolution was fixed at 3 hr for all slags except the experiments on dependence on holding time. Hydrogen contents of CaO-SiO₂ slags are shown in Fig. 3. A minimum was observed near the composition of metasilicate. Infrared absorption spectra of these slags are shown in Fig. 4. Two absorptions were observed at 2.9 μ (Band 1) and 3.5 μ (Band 2). With increasing CaO/SiO₂ ratio, band 2 appeared more clearly. In order to obtain the infrared absorption due to only hydrogen absorption, the slag produced in nitrogen was selected as the standard slag without hydrogen. That is, the infrared absorption spectra due to hydrogen absorption were determined by subtracting the

Fig. 2 Hydrogen contents in $0.4\text{CaO} \cdot 0.6\text{SiO}_2$ slags plotted against absorption time (at 1600°C , $P_{\text{H}_2\text{O}} = 0.128 \text{ atm.}$).Fig. 3 Dependence of hydrogen content in lime silicate slags upon slag composition (at 1600°C , $P_{\text{H}_2\text{O}} = 0.128 \text{ atm.}$).

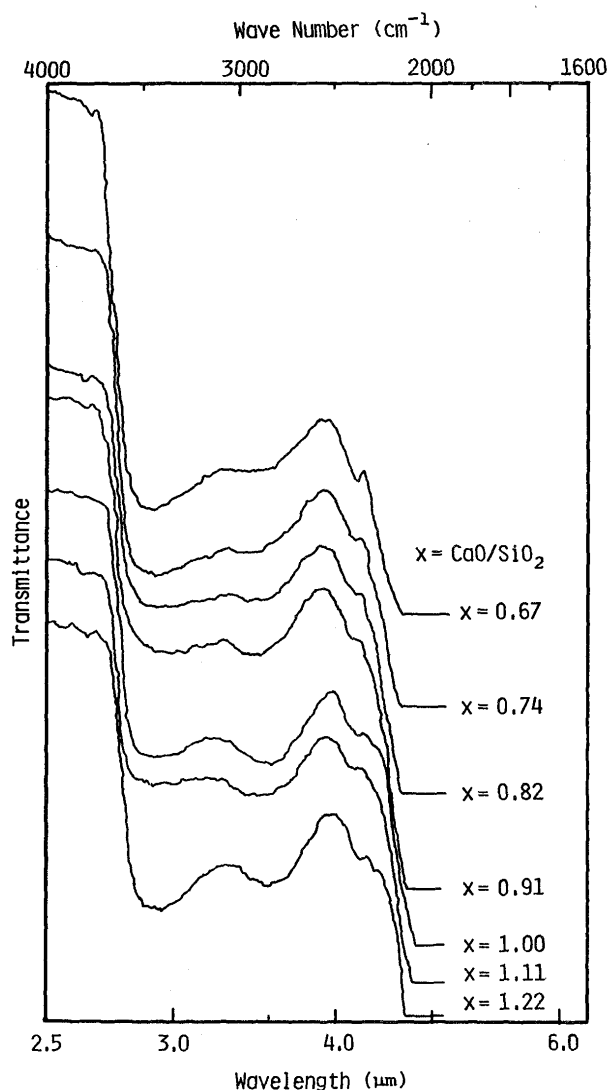


Fig. 4 Infrared absorption spectra of lime silicate slags.

standard infrared absorption from the infrared absorption of each slag. The standard spectrum of the slag produced in nitrogen and a few spectra obtained by subtracting method are shown in Figs. 5 and 6. Subsequently, these spectra were resolved into three spectra by computer calculation after the intensity unit of these spectra was transformed into absorbance using Lambert-Beer formula. A typical resolved spectrum is shown in Fig. 7. The ratios of the areas of three spectra to total area were also determined as shown in Fig. 8. Band 1 near 2.9μ showed a minimum near metasilicate composition whereas a maximum was observed at the similar slag composition in the case of band 2 near 3.4μ . Fig. 9 shows DTA curves obtained from a few hydrogen-absorbed slags. Two peaks were observed near 380°C and the temperature between 800°C and 900°C , respectively. A small peak appeared near 500°C in the basic slag with $\text{CaO/SiO}_2 = 55/45$.

3.2 CaF_2 - CaO - SiO_2 ternary slag

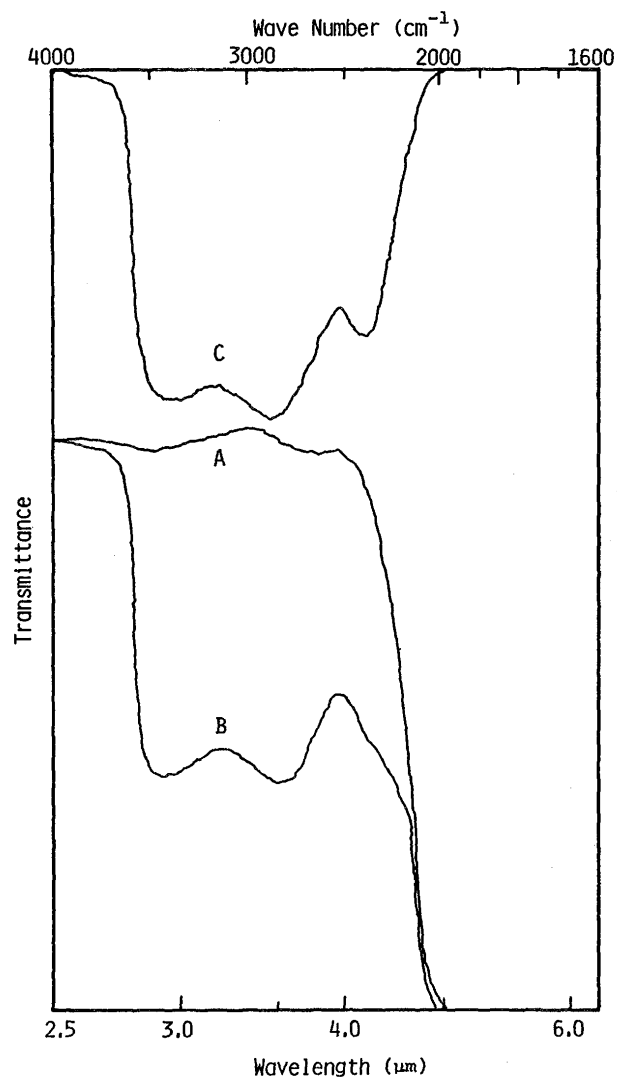


Fig. 5 Infrared absorption spectra of lime metasilicate slags produced under N_2 and $\text{Ar} + \text{water vapor}$. A ; under N_2 atmosphere, B ; under $\text{Ar} + \text{water vapor}$ ($\text{P}_{\text{H}_2\text{O}} = 0.128 \text{ atm.}$) C ; A-B

Hydrogen contents in calcium fluorosilicate slags with 5 mol% and 10 mol% CaF_2 (initial contents) are given in Fig. 10. Hydrogen contents in acidic slags increased as the result of CaF_2 addition to parent CaO-SiO_2 slags although final CaF_2 content was very small in each slag as shown in Table 1. On the contrary, hydrogen contents in basic slags were inclined to decrease or unchangeable, compared with those of CaO-SiO_2 slags with the same CaO/SiO_2 ratio. Infrared absorption spectra of fluorosilicate slags with 5 mol% and 10 mol% CaF_2 (initial contents) are shown in Figs. 11 and 12. Relative intensity of band 2 to band 1 was inclined to increase with increasing CaO/SiO_2 ratio until the ratio reaches unit. Infrared absorption spectra of the slags with constant SiO_2 content (60 mol%) were also measured and the result is given in Fig. 13. In these slags, the intensity of band 2 increased with increasing initial CaF_2 content. Increase

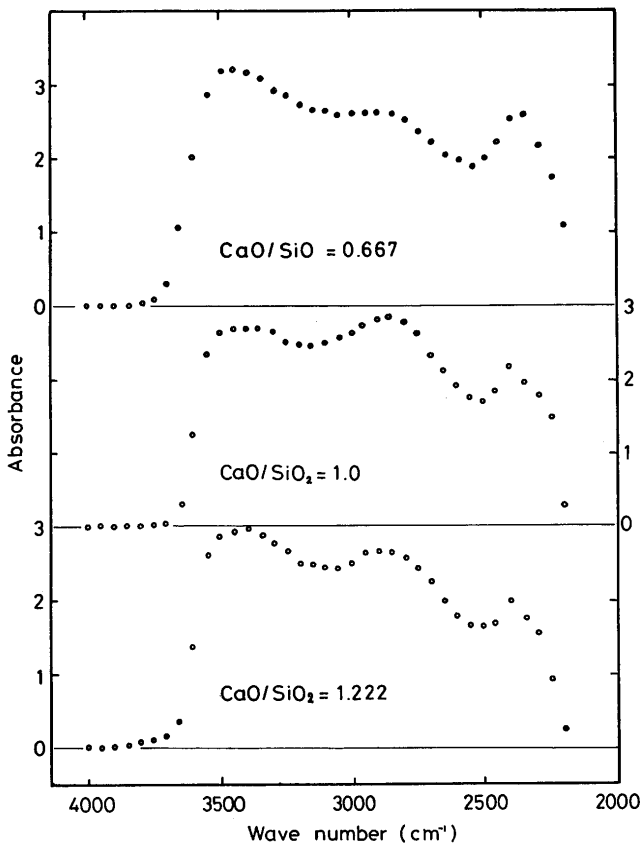


Fig. 6 Infrared absorption spectra of a few lime silicate slags expressed by absorbance unit.

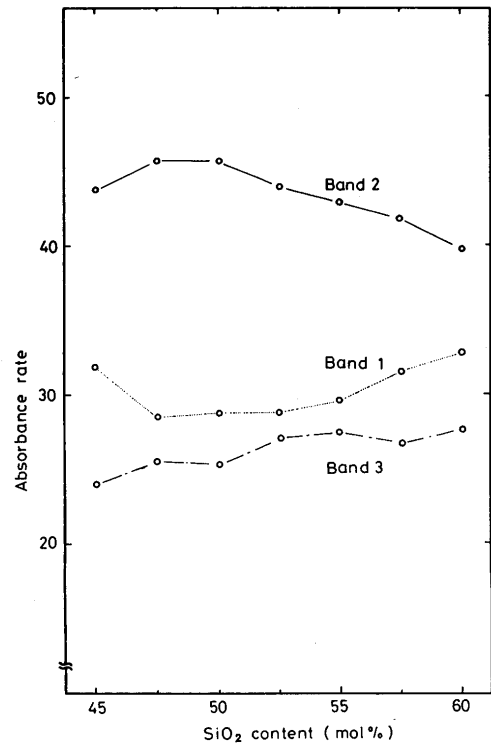


Fig. 8 Dependence of the ratio of each band in absorbance unit upon SiO₂ content.

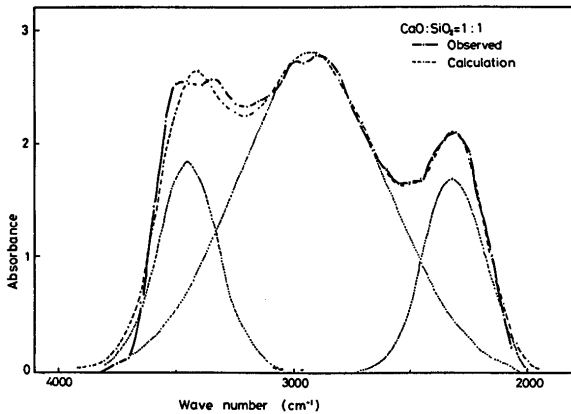


Fig. 7 A typical infrared spectrum of lime silicate slag resolved into three Gaussian bands.

of the intensity of band 2 was also observed in the result of time-dependence of hydrogen content in the slags with the initial CaF₂ content of 25 mol%. Further, hydrogen contents in these slags were less than those in the slags with same CaO/SiO₂ ratio and no CaF₂ until reaction time reached about 1 hr. These results are shown in Figs. 14 and 15. When reaction time was over 90 min, hydrogen content became higher than those in the CaO-SiO₂ slags with the same CaO/SiO₂ ratio.

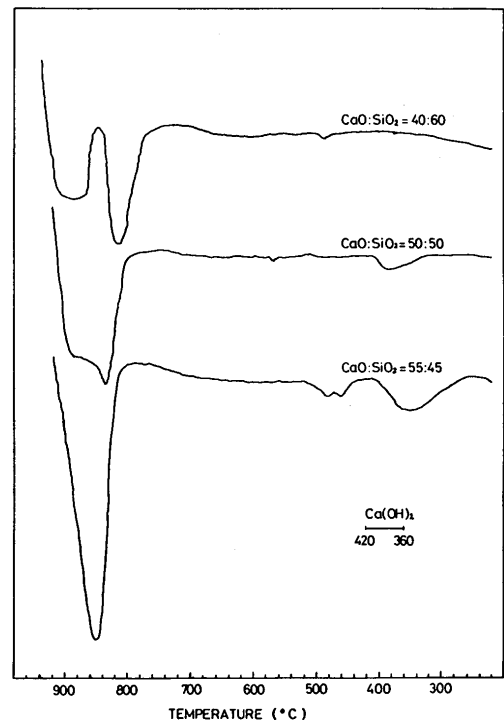


Fig. 9 DTA curves of a few lime silicate slags.

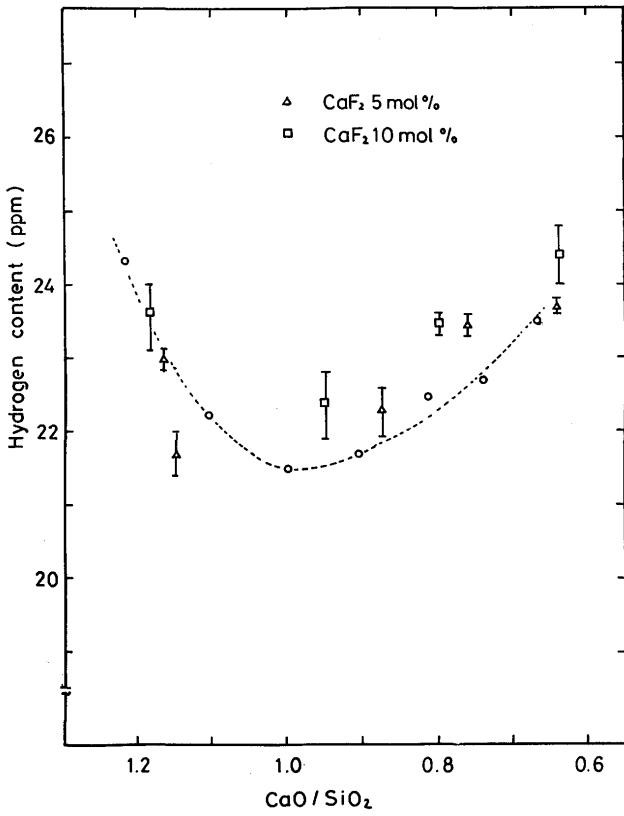


Fig. 10 Hydrogen contents of calcium fluorosilicate slags added 5 mol% and 10 mol% CaF_2 as initial content.

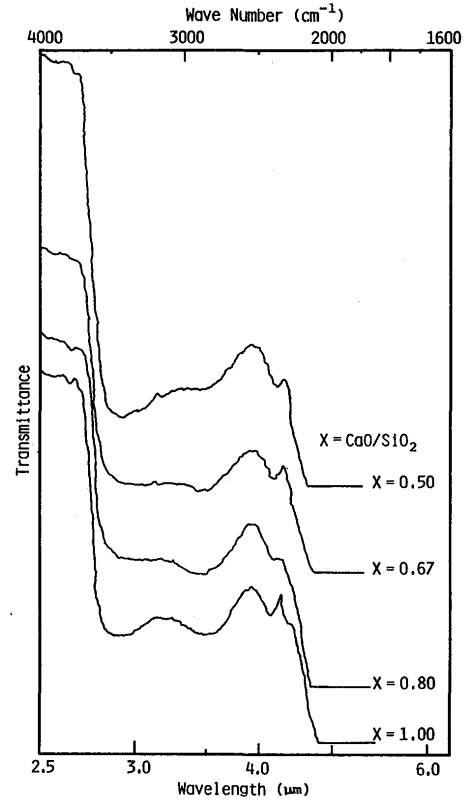


Fig. 12 Infrared absorption spectra of calcium fluorosilicate slags added 10 mol% CaF_2 as initial content.

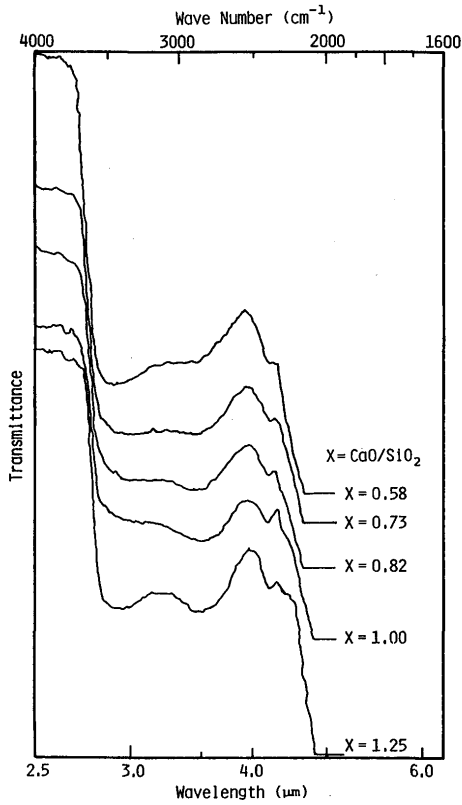


Fig. 11 Infrared absorption spectra of calcium fluorosilicate slags added 5 mol% CaF_2 as initial content.

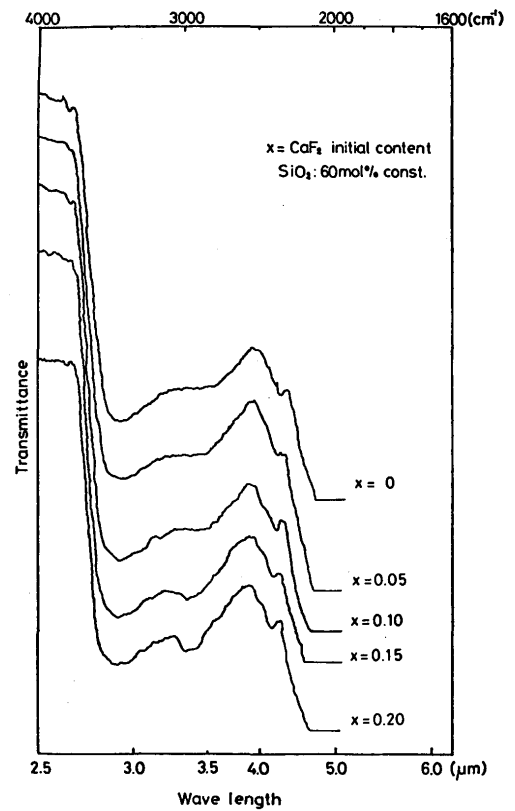


Fig. 13 Infrared absorption spectra of calcium fluorosilicate slags with constant SiO_2 (60 mol%).

Table 1 Initial and final slag compositions of calcium fluorosilicates and hydrogen content in these slags

Specimen No.	Initial Composition (mol%)			Final Composition (mol%)			Hydrogen Content (ppm)
	CaO	SiO ₂	CaF ₂	CaO	SiO ₂	CaF ₂	
1	35.0	60.0	5.0	39.3	60.7	0.07	23.7
2	40.0	55.0	5.0	44.1	55.9	0.03	23.5
3	42.8	52.2	5.0	46.4	53.6	0.02	22.3
4	47.5	47.5	5.0	53.6	46.4	0.01	21.6
5	50.0	45.0	5.0	53.7	46.2	0.10	23.0
6	30.0	60.0	10.0	39.0	46.2	0.10	24.4
7	36.0	54.0	10.0	44.5	55.5	0.03	23.5
8	40.0	50.0	10.0	48.9	51.1	0.01	22.4
9	45.0	45.0	10.0	54.2	45.7	0.04	23.6
10	40.0	60.0	—	—	—	—	23.5
11	35.0	60.0	5.0	39.3	60.7	0.07	23.7
12	30.0	60.0	10.0	39.0	60.9	0.10	24.4
13	25.0	60.0	15.0	42.0	57.9	0.08	25.5
14	20.0	60.0	20.0	40.0	59.9	0.07	26.0

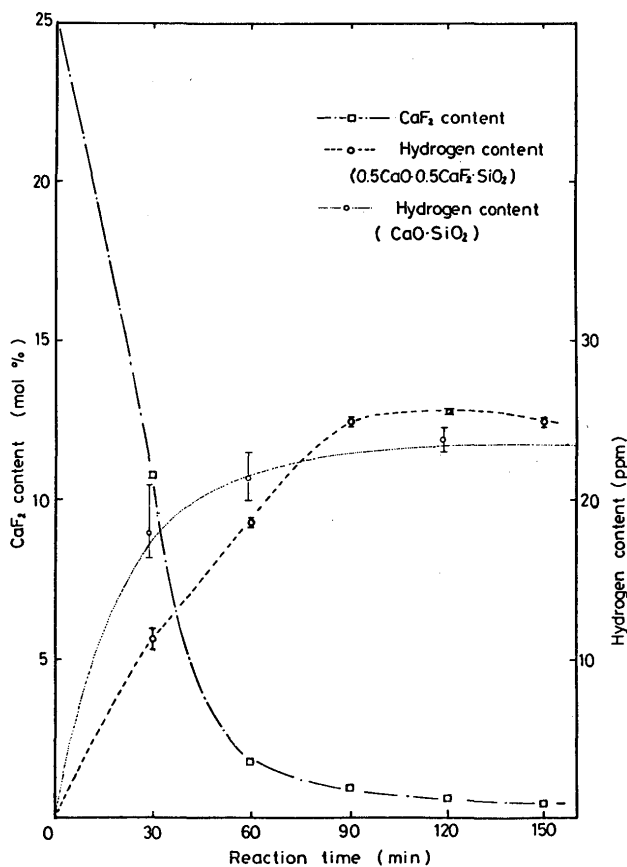


Fig. 14 Hydrogen and CaF₂ contents in calcium fluorosilicate slags plotted against reaction time.

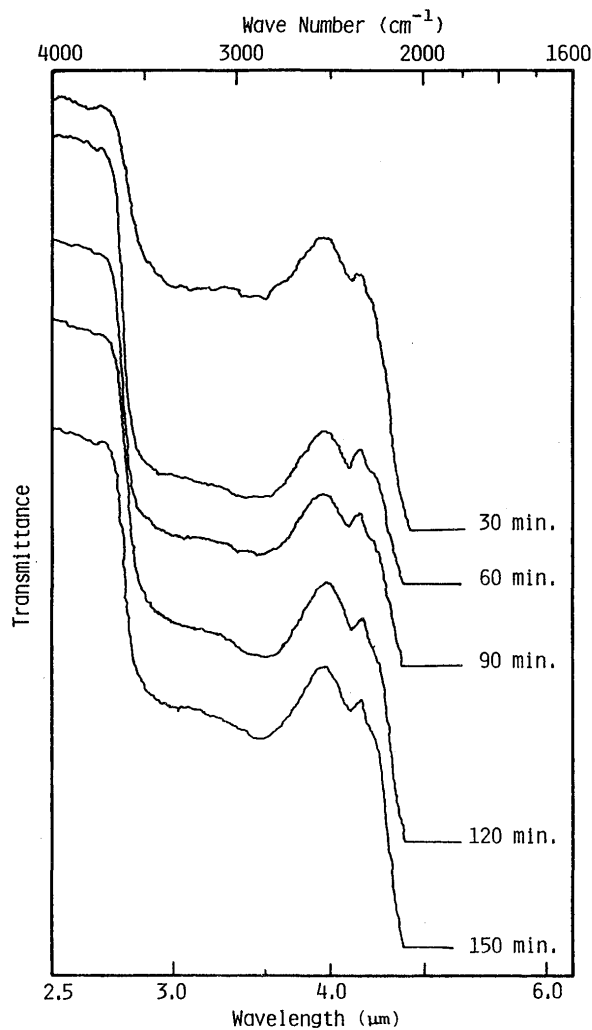


Fig. 15 Dependence of infrared absorption spectra of 0.5 CaF₂ · 0.5 CaO · SiO₂ slags upon reaction time.

4. Discussion

The observation of three absorptions at 2.9μ , 3.5μ and 4.3μ , as shown in Fig. 6, indicates that there are three states of hydrogens in lime silicate slags. Taking into account the previous papers,^{5) - 8)} it is concluded that these absorptions are attributed to the stretching vibrations of three different hydroxyls in these slags. Infrared absorptions due to water vapor and liquid water are observed at 2.77μ and 3.0μ , respectively.^{9), 10)} The shift of the absorption of liquid water can be originated from hydroxyl with hydrogen bond. The shift of the absorption due to stretching vibration of hydroxyl can be explained under the assumption that a hydroxyl in a Morse-type potential field is subjected to a suitable electric field. That is, if the electric field of 6.5×10^5 esu or so is applied to a hydroxyl in a Morse-type potential field, the absorption due to the stretching vibration of hydroxyl can easily shift to about 2.9μ .¹¹⁾ On the other hand, Lippincott related the shift of the infrared absorption of hydroxyls in various materials with the distance between oxygens ($O \cdots O$ distance) in hydrogen-bonded hydroxyl ($OH \cdots O$) using a different potential from Morse-type one.¹²⁾ According to the result, the shift of the absorption due to the stretching vibration of hydrogen-bonded hydroxyl increased with decreasing $O \cdots O$ distance. Comparing the hydroxyl affected by electric field with the one in Lippincott's model, the former corresponds to the latter with long $O \cdots O$ distance. Thus, it is concluded that the three infrared absorptions are attributed to the three sorts of hydrogen-bonded hydroxyls with different $O \cdots O$ distances. That is, absorption bands 1, 2 and 3 observed in CaO-SiO₂ slags can be assigned to nearly free hydroxyl affected by an electric field, hydrogen-bonded hydroxyls with intermediate and short $O \cdots O$ distances, respectively. According to the calculation by Lippincott, these $O \cdots O$ distances in three hydroxyls become 2.95 \AA (for band 1), 2.65 \AA (for band 2) and 2.55 \AA (for band 3).

From the results shown in figs. 3 and 8, dependency of total hydrogen content upon slag composition does not relate to band 2 but predominantly to band 1. According to structural theories of silicate melt,^{13) - 17)} bridged oxygen content increases abruptly near meta-silicate composition in CaO-SiO₂ slag whereas free oxygen content decreases near the same composition. Therefore, it is suggested that total hydrogen content increases by the formation of hydroxyl which is related with free oxygen in basic composition or with bridged oxygen in acidic composition, respectively.

Three sorts of hydrogen sites in CaO-SiO₂ slag can be determined from $O \cdots O$ distance in hydrogen-bonded hydroxyl and dependencies of three absorption bands on slag composition. Firstly, it is suggested that nearly free

hydroxyl can be formed as the result of trapping in a few sorts of interstices in silicate networks because the hydroxyl has the long $O \cdots O$ distance of 2.95 \AA and its content in acidic composition decreased with decreasing SiO₂ content. Assuming the closed-packing quasi-lattice of oxygen, three sorts of interstices surrounded by 4, 6 and 9-12 oxygens can be formed in silicate. The two former interstices can not be suitable to the site for hydrogen in nearly free hydroxyl on account of following reasons;

- (1) $O \cdots O$ distance is very short in the interstice surrounded by four oxygens.
- (2) band 1 was strongly observed in the slags containing TiO₂ and Al₂O₃.^{7), 18)}
- (3) the bond angle of $OH \cdots O$ is inclined to become straight.

Therefore, it can be considered that nearly free hydroxyl producing band 1 is formed in the interstice surrounded by oxygens from 9 to 12, that is, so-called pocket in silicate network. If nearly free hydroxyl is located in the pocket, it is expected that the intensity of band 1 decreases with increasing oxygen density of silicate because the quantity of the pocket is reversely proportional to oxygen density of silicate¹⁹⁾. Practically, oxygen density of CaO-SiO₂ slag in acidic region increases with decreasing SiO₂ content, so that the behavior of band 1 in acidic region can be well explained by oxygen density of slag. The exothermic peak near 380°C in DTA curves showed a good agreement with that of Ca(OH)₂ and its intensity became larger with increasing CaO/SiO₂ ratio as shown in fig. 9. Accordingly, it is reasonable to ascribe the increase of intensity of band 1 to the formation of nearly free hydroxyl associated with Ca²⁺ ion such as Ca(OH)₂ or Ca²⁺(OH)⁻O⁻.

The $O \cdots O$ distance in hydrogen-bonded hydroxyl producing band 2 is about 2.65 \AA .¹²⁾ The shortest $O \cdots O$ distance becomes about 3.2 \AA among those formed by oxygens surrounding interstices in silicate. From molar refraction values of bridged and non-bridged oxygens²⁰⁾,²¹⁾ the ionic radius of bridged oxygen becomes 1.19 \AA and that of non-bridged oxygen lies between 1.27 \AA and 1.30 \AA . Therefore, band 2 is not ascribed to a hydrogen-bonded hydroxyl in an interstice in silicate but to the hydroxyl of $OH \cdots O^-$ type.

Some investigators suggested that band 3 is originated from strongly hydrogen-bonded hydroxyl.^{5), 6)} As shown in fig. 8, relative quantity of hydroxyl related to band 3 increased with increasing SiO₂ content. The hydroxyl has the very short $O \cdots O$ distance of 2.55 \AA . Taking into account ionic radii of bridged and non-bridged oxygens, the $O \cdots O$ distance in the hydroxyl of $OH \cdots O^-$ type becomes shorter than that in the hydroxyl of $OH \cdots O^-$

type. Thus, it would be reasonable to assign band 3 to the hydroxyl of $\text{OH} \cdots \text{O}^\ominus$ type.

Structures of three sorts of hydroxyls in lime fluorosilicate slags are fundamentally in the similar states because infrared absorptions in fluorosilicate slags were observed at similar positions to those in silicate slags. In the case of lime fluorosilicate slags with high initial content of CaF_2 , as shown in figs. 13 and 15, the intensity of band 2 increased with decreasing actual CaF_2 content. Further, total hydrogen content in fluorosilicate slag became lower than that in silicate slag with the same CaO/SiO_2 ratio when slag contains about 7 mol% CaF_2 at least. These results are closely related to the breaking effect of CaF_2 on silicate network. The formation of Si-F and Ca-F bonds in calcium fluorosilicate slag was supported by spectroscopic investigations such as ESCA and X-ray emission fine feature analysis²²). Further, it was indicated that Ca-F bond can be predominantly formed more than 7-10 mol% CaF_2 whereas Si-F bond can be formed less than the same content of CaF_2 . Thus, active non-bridged oxygen can be formed as the result of producing Si-F bond when CaF_2 content become less than about 7 mol%. Therefore, the hydroxyl $\text{OH} \cdots \text{O}^\ominus$ relating to band 2 can be produced by the formation of active non-bridged oxygen and total hydrogen content in fluorosilicate slag become higher than that in silicate slag. Breaking effect on silicate network by CaF_2 addition becomes smaller as slag becomes more basic, so that it can be explained that total hydrogen content becomes similar to that in silicate with $\text{CaO}/\text{SiO}_2 = 1$ or over. Conclusively, it can be considered that fluoride addition is effective on lowering hydrogen absorption into fluorosilicate slag as far as fluorine ion is in the form of M-F bond (M : modifier cation) in the slag.

5. Summary

Hydrogen absorption of lime silicate and fluorosilicate slags and state of hydrogen in these slags were investigated by gas chromatric analysis using impulse fusion method and infrared absorption spectroscopy. In lime silicate slags, a minimum was observed near metasilicate composition. Infrared absorption spectrum of each slag due to only hydrogen absorption was determined by subtracting the standard absorption, whose spectrum was obtained from the slag produced in nitrogen, from the absorption of each slag. These absorption spectra were resolved into three absorption bands of Gaussian type by computer calculation. These three bands were observed at 2.9 μ (band 1), 3.4 μ (band 2) and 4.3 μ (band 3), respectively. They were assigned to nearly free hydroxyl, hydroxyls of $\text{OH} \cdots \text{O}^\ominus$ and $\text{OH} \cdots \text{O}^\circ$ types from the dependence of

each band on slag composition with the aid of structural consideration on silicate.

CaF_2 addition to calcium silicate was effective to lowering hydrogen absorption of the slags when actual content of CaF_2 in slag was more than about 7 mol%. When actual CaF_2 content became less than about 7 mol%, however, CaF_2 addition showed harmful effect to lowering hydrogen content in slag. It was interpreted that the harmful effect is attributed to the formation of active non-bridged oxygen produced by the formation of Si-F bond in slag. Conclusively, it was suggested that the addition of fluoride to silicate slag is effective on lowering hydrogen absorption into slag as far as fluorine ion is bonded to modifier cation.

References

- 1) R.W.Lee, R.C.Frank and D.E.Swets; *J. Chem. Phys.*, **36** (1962), p. 1062.
- 2) R.W.Lee and D.L.Fry: *Phys. Chem. Glasses*, **7** (1966), p. 19.
- 3) T.Fuwa, S.Banya, T.Fukushima and Y.Iguchi: *Tetsu to Hagane*, **53** (1967), p. 91 (in Japanese).
- 4) Y. Iguchi, S. Banya and T. Fuwa: *Trans. ISIJ.*, **9** (1969), p. 189.
- 5) V.H. Scholze: *Glastech. Ber.*, **36** (1963), p. 347.
- 6) R.V. Adams: *Phys. Chem. Glasses*, **2** (1961), p. 39.
- 7) V.H. Scholze: *Glastech. Ber.*, **32** (1959), p. 81.
- 8) M. Imai, H. Ooi and T. Emi: *Tetsu to Hagane*, **50** (1964), p. 878 (in Japanese).
- 9) L.G. Bonner: *Phys. Rev.*, **46** (1934), p. 458.
- 10) J.J. Fox and A.E. Martin: *Proc. Roy. Soc.* **174A** (1940), p. 234.
- 11) N.D. Coggeshall: *J. Chem. Phys.* **18** (1950), p. 987.
- 12) E.R. Lippincott and R. Schroeder: *ibid.*, **23** (1955), p. 1099.
- 13) S.G. Whiteway, I.B. Smith and C.R. Masson: *Can. J. Chem.*, **48** (1970), p. 34.
- 14) C.R. Masson, I.B. Smith and S.G. Whiteway: *ibid.*, **48** (1970), p. 1456.
- 15) M.L. Kapoor, G.M. Mehrotra and M.G. Froberg: *Arch. Eisenhüttenwes.*, **45** (1974), p. 213.
- 16) M.L. Kapoor, G.M. Mehrotra and M.G. Froberg: *ibid.*, **45** (1974), p. 663.
- 17) D.R. Gaskell: *Met. Trans.* **8B** (1977), p. 131.
- 18) V.H. Scholze: *Glastech. Ber.*, **32** (1959), p. 142.
- 19) E.D. Lacy: "The Vitreous State" *The Glass Delegacy*, University of Scheffield (1955).
- 20) S.S. Batzanov: "Refractometry and Chemical Structure" Van Nostrand Co., (1966).
- 21) N. Iwamoto and Y. Makino: *J. Non-Crystalline Solids*, **34** (1979), p. 381.
- 22) N. Iwamoto and Y. Makino: *J. Non-Cryotalline Solids*, in press.